PHYSICAL REVIEW D **79,** 015015 (2009)

Signals of inert doublet dark matter in neutrino telescopes

Prateek Agrawal,[1] Ethan M. Dolle,[2] and Christopher A. Krenke[1,2]
[1]*Department of Physics, University of Maryland, College Park, Maryland 20742, USA*
[2]*Department of Physics, University of Arizona, Tucson, Arizona 85721, USA*
(Received 18 November 2008; published 28 January 2009)

One of the simplest extensions of the standard model that explains the observed abundance of dark matter is the inert doublet model. In this theory a discrete symmetry ensures that the neutral component of an additional electroweak doublet scalar is stable and constitutes a dark matter candidate. As massive bodies such as the Sun and Earth move through the dark matter halo, dark matter particles can become gravitationally trapped in their cores. Annihilations of these particles result in neutrinos, which can potentially be observed with neutrino telescopes. We calculate the neutrino detection rate at these experiments from inert doublet dark matter annihilations in the cores of the Sun and the Earth.

DOI: 10.1103/PhysRevD.79.015015 PACS numbers: 95.35.+d, 12.60.−i, 12.60.Fr

I. INTRODUCTION

One of the most pressing questions currently in physics is the nature of dark matter. It is known that most of the matter in the Universe is comprised of nonluminous (dark), neutral matter. Moreover, it is also known that none of the standard model particles can be the dark matter. Hence, to explain dark matter, we must introduce new physics beyond the standard model. The most appealing scenario from a cosmological standpoint is that of a weakly interacting massive particle (WIMP). The WIMP is theoretically attractive because any weakly interacting particle with a mass in the TeV scale will give approximately the correct relic abundance of dark matter. Many extensions of the standard model contain such dark matter candidates, for example, supersymmetry [1], extra dimensions [2,3], and little Higgs [4].

Dark matter is distributed across the galaxy in the form of a halo. As the dark matter particles interact with nuclei in large objects such as the Sun or Earth, a certain fraction of the scattered dark matter particles will not have enough kinetic energy to escape the gravitational pull of the object. Thus, eventually a build up of dark matter will occur in the cores of massive objects. The dark matter particles will then annihilate, producing standard model particles, which eventually decay to neutrinos. If the neutrinos originate from the cascade of a TeV scale object such as a WIMP, they will typically have an energy of a few hundred GeV. This energy range is detectable in neutrino telescopes such as IceCube. This idea has been investigated before in the context of supersymmetric dark matter [5] and Kaluza-Klein dark matter candidates [6].

In this paper, we consider the possible signal in neutrino telescopes from dark matter annihilations in the Sun and Earth for the inert doublet model (IDM). In this model, the Higgs sector of the standard model (SM) is extended to include an additional $SU(2)$ doublet that does not acquire a vacuum expectation value. If an additional Z_2 symmetry is imposed, the neutral particle in the additional doublet becomes stable and thus, a dark matter candidate. The possible neutrino signal from the inert doublet model is especially interesting because this type of dark matter arises in extensions of the SM motivated by the little hierarchy problem, such as the left-right twin Higgs model [7].

The format of the paper is as follows: In Sec. II we discuss the basics of the IDM and list some constraints. In Sec. III we discuss the dynamics of capture of dark matter particles by massive objects and calculate the capture and annihilation rates for the Sun and Earth for the inert doublet model. In Sec. IV, we discuss the determination of the detector rate. In Sec. V we present our results, and in Sec. VI we conclude.

II. THE INERT DOUBLET MODEL

The inert doublet model consists of the standard model with an additional electroweak doublet scalar, H_2, with the same quantum numbers as the SM Higgs. This doublet is odd under a Z_2 symmetry, while all other fields are even, and does not acquire a vacuum expectation value. Hence, H_2 couples only to SM gauge bosons, the SM Higgs, and itself. Since H_2 is odd under the Z_2 symmetry, this ensures that the lightest component of H_2 is stable. Thus, if the neutral scalar is lighter than the charged scalar in H_2, it is a good dark matter candidate [7,8].

The general pattern of symmetry breaking in a two Higgs doublet model was first investigated by Deshpande and Ma [9]. Recently, Barbieri *et al.* have shown that in the case of an unbroken Z_2 and appropriately chosen splittings the model passes electroweak precision tests with a heavy Higgs, thus solving the little hierarchy problem [10]. They refer to this case as the inert doublet model since the new Higgs doublet cannot couple to fermions. The IDM has been shown to give the correct relic abundance for dark matter [11]. The direct detection rates of dark matter in this model were examined by [12]. It has also been analyzed for indirect signals of dark matter via photons [13] and mono-

chromatic photon production at the Galactic center [14]. The LEP II analysis for neutralino pair production has recently been translated into constraints on the IDM [15].

A. Parametrization of the potential

The most general potential consistent with the Z_2 symmetry is

$$V = \mu_1^2|H_1|^2 + \mu_2^2|H_2|^2 + \lambda_1|H_1|^4 + \lambda_2|H_2|^4 + \lambda_3|H_1|^2|H_2|^2 + \lambda_4|H_1^\dagger H_2|^2 + \frac{\lambda_5}{2}\{(H_1^\dagger H_2)^2 + \text{H.c.}\}. \quad (1)$$

Expanding the potential above in unitary gauge,

$$H_1 = \begin{pmatrix} 0 \\ (v+h)/\sqrt{2} \end{pmatrix}, \quad (2)$$

$$H_2 = \begin{pmatrix} H^+ \\ (S+iA)/\sqrt{2} \end{pmatrix}, \quad (3)$$

we obtain,

$$\begin{aligned} m_h^2 &= 2v^2\lambda_1 = -2\mu_1^2 \\ m_S^2 &= \mu_2^2 + \tfrac{1}{2}(\lambda_3+\lambda_4+\lambda_5)v^2 \\ m_A^2 &= \mu_2^2 + \tfrac{1}{2}(\lambda_3+\lambda_4-\lambda_5)v^2 \\ m_{H^\pm}^2 &= \mu_2^2 + \tfrac{1}{2}\lambda_3 v^2. \end{aligned} \quad (4)$$

This leaves us with seven independent real parameters: μ_1, μ_2, λ_1, λ_2, λ_3, λ_4, and λ_5. Fixing the Z mass fixes v, while fixing the SM Higgs mass fixes μ_1 and λ_1. Following [10] we define $\lambda_L = (\lambda_3+\lambda_4+\lambda_5)$. Fixing the scalar mass and the mass splittings between the scalar, pseudoscalar, and charged particles as m_S, $\delta_1 = m_{H^\pm} - m_S$, and $\delta_2 = m_A - m_S$ fixes μ_2, λ_3, and λ_5. This leaves us with the new parameter set: m_Z, m_h, λ_2, λ_L, δ_1, δ_2, and m_S. The Z mass is fixed by LEP, while we take $\lambda_2 = 0.1$ [13]. This parameter does not affect the neutrino flux rate calculation directly.

B. Constraints

There are a number of constraints that serve to limit our parameter space. We discuss each of them in detail below.

1. From Ωh^2

Recent measurements from WMAP have led to a precise determination of the amount of dark matter in the Universe: $\Omega_{\rm DM}h^2 = 0.112 \pm 0.009$ [16]. The program micrOMEGAs [17] uses a calcHEP [18] model file to solve the Boltzman equation numerically to find the relic density. We used this to exclude a large portion of the parameter space. Two regions are consistent with WMAP at the 3σ level: a low mass region, where $m_S < 100$ GeV, and a high mass region, where 500 GeV $< m_{H_0} <$ 2 TeV.

2. From direct detection bounds

The direct detection bounds put a constraint on the value of λ_5. As $\lambda_5 \to 0$, the neutral scalar S and the pseudoscalar A become degenerate. In this case, these particles can scatter off matter via a Z exchange, giving cross sections eight to nine orders of magnitude larger than present direct detection bounds [19]. This constraint can be avoided if the mass splitting between S and A is higher than the kinetic energy of dark matter in the halo, or $\delta_2 \sim$ a few hundred MeV.

3. From Γ_Z

Data from LEP has put tight constraints on the width of the Z boson, such that new decay channels are very restricted. This puts lower bounds on the scalar mass and the mass splittings.

$$m_S + m_A > m_Z \Rightarrow m_S > \frac{m_Z - \delta_2}{2},$$
$$2m_{H^\pm} > m_Z \Rightarrow m_S > \frac{m_Z - 2\delta_1}{2}.$$

4. From model stability

In order to ensure stability of the model, we require λ_L, $\lambda_3 > -2\sqrt{\lambda_1\lambda_2}$. Since we consider the scalar, S, to be the dark matter candidate, $\lambda_L < \lambda_3$, and the first condition is sufficient. Substituting the SM Higgs mass for λ_1 yields the condition $\lambda_L > -\frac{2m_h}{v}\sqrt{\frac{\lambda_2}{2}}$. For a modest choice of λ_2 and m_h, this excludes almost all negative λ_L couplings.

III. DARK MATTER CAPTURE AND ANNIHILATION

Dark matter particles (DMPs) accumulate in the massive bodies from the Galactic halo, and are depleted by annihilations. Given a long enough time, this process can come into equilibrium. The differential equation governing the number of DMPs in the Sun (or Earth) is

$$\dot{N} = C - C_A N^2. \quad (5)$$

Here C is the capture rate from the halo, and $C_A = \langle\sigma_A v\rangle V_2/V_1^2$. $\langle\sigma_A v\rangle$ is the total cross section times the relative velocity in the limit $v \to 0$. V_j are the effective volumes for the Sun and Earth, given by

$$V_j = (3m_{\rm pl}^2 T/(2jm_S\rho))^{3/2}, \quad (6)$$

and $m_{\rm pl}$ is the Planck mass, T is the temperature, and ρ the core density of the massive body. Equation (5) can be solved to obtain the annihilation rate of DMPs

$$\Gamma_A = \tfrac{1}{2}C\tanh^2(t/\tau). \quad (7)$$

If the time scale for equilibriation ($\tau = \sqrt{CC_A}$) is much smaller than the age of the solar system (t), then Γ_A is

simply $\frac{1}{2}C$. Since this is the scenario of a maximal signal, this indicates that the capture rate is the dominant factor in determining the magnitude of the signal.

A. Capture rate

The capture rate depends on the DMP scattering cross section from the nuclei. The calculation of the cross section proceeds in three steps. First we calculate the partonic cross section with quarks and gluons. We next translate this into the interaction with nucleons, by taking the quark/gluon matrix elements in the nucleonic state. Finally, we evaluate the nucleon operator matrix elements in the nucleus [20]. Since these particles are nonrelativistic, the cross section calculation is greatly simplified. The DMP undergoes scalar interactions which coherently add in the nucleus, and hence it couples to the mass of the nucleus. The elastic cross section at zero momentum transfer is [10]

$$\sigma_0^i = \frac{m_S^2 m_{N_i}^2}{4\pi(m_S + m_{N_i})^2}\left(\frac{\lambda_L}{m_S m_h^2}\right)^2 f^2 m_{N_i}^2 \tag{8}$$

Here, m_N is the mass of the nucleus and $f \sim 0.3$ is the nucleonic matrix element [21], defined by

$$\langle N|\sum m_q q\bar{q}|N\rangle = f m_N \langle N|N\rangle. \tag{9}$$

At a finite momentum transfer, the particle does not see the entire nucleus, and hence the cross section is suppressed by a form factor ($F_i(m_S)$). Other factors that influence the capture rate are the elemental abundance f_i, distribution ϕ_i, and the kinematic suppression, $S(m_s/m_{N_i})$ [22]. The capture rate is given by

$$C = c\frac{\rho_{0.3}}{(m_S/\mathrm{GeV})\bar{v}_{270}}\sum_i F_i(m_S) \times\left(\frac{\sigma_0^i}{10^{-4}\ \mathrm{pb}}\right) f_i \phi_i \frac{S(m_S/m_{N_i})}{(m_{N_i}/\mathrm{GeV})}, \tag{10}$$

where $c = 4.8 \times 10^{24}\ \mathrm{s}^{-1}$ for the Sun and $c = 4.8 \times 10^{15}\ \mathrm{s}^{-1}$ for Earth, $\rho_{0.3}$ is the local halo mass density in units of 0.3 GeV cm^{-3}, and $\bar{v}_{270}$ is the dark matter velocity dispersion in terms of 270 km s^{-1}. The quantities f_i and ϕ_i for the Sun and Earth are given in [23] The sum is over all elements in the Sun or Earth. The kinematic suppression factor can be parametrized as follows:

$$S(x) = [A^{3/2}/(1 + A^{3/2})]^{2/3}, \tag{11}$$

$$A = \frac{3}{2}\frac{x}{(x-1)^2}\left(\frac{\langle v_{\mathrm{esc}}\rangle^2}{\bar{v}^2}\right). \tag{12}$$

The mean escape velocity, $\langle v_{\mathrm{esc}}\rangle$ is obtained by numerical fitting to the exact kinematic suppression. For the Sun, $\langle v_{\mathrm{esc}}\rangle = 1156$ km s^{-1}, and for the Earth $\langle v_{\mathrm{esc}}\rangle = 13.2$ km s^{-1}. This factor arises from the fact that in order to be captured, the scalar has to scatter off a nucleus with a velocity less than the escape velocity in that object. If the mass of the nucleus is equal to the mass of the scalar, then it can potentially lose all its kinetic energy in an elastic collision. It can be seen from the parametrization above that the capture is suppressed more if the mass of the dark matter particles is very different from the mass of the nucleus. The form factor suppression can be modeled numerically for simplicity. For the Earth, the only appreciable effect is the suppression from iron, so $F_i(m_S) \simeq 1$ for all other elements. For iron,

$$F_{\mathrm{Fe}} \simeq 1 - 0.26\left(\frac{A}{A+1}\right). \tag{13}$$

For the Sun, the fitting is slightly more complicated. The suppression is given by

$$F_i(m_S) = F_i^{\mathrm{inf}} + (1 - F_i^{\mathrm{inf}})\exp\left[-\left(\frac{\log(m_s)}{\log(m_c^i)}\right)^{\alpha_i}\right]. \tag{14}$$

The quantities F_i^{inf}, m_c^i, and α_i are numerical fitting parameters taken from [23].

B. Annihilation

These accumulated DMPs can annihilate into standard model particles. Subsequently, these particles can decay

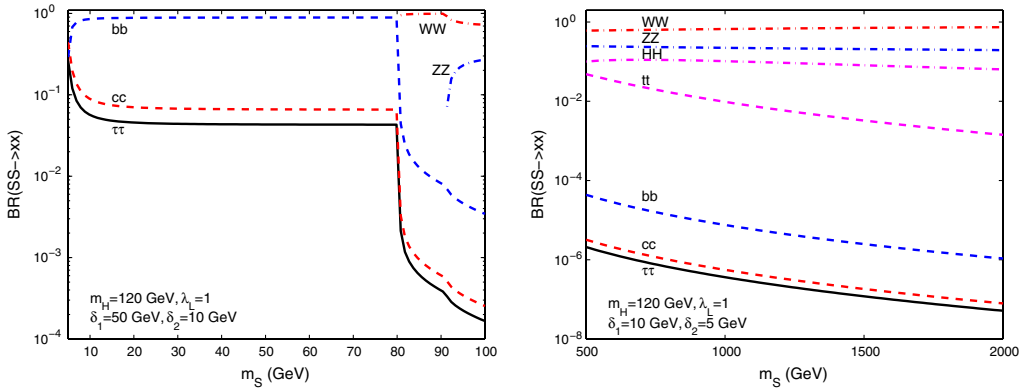

FIG. 1 (color online). Branching Fractions of S into SM particles for low mass region (left) and high mass region (right).

into energetic muon neutrinos and hence be detected in astrophysical neutrino detectors. The scalar S usually annihilates into a two-body state, and hence the typical energy of the neutrino is $\simeq \frac{1}{4} m_S$.

The overall annihilation rate in the Sun or Earth is essentially set by the capture rate (assuming near maximal signal). We calculate the dark matter annihilation branching fractions into various standard model particles. We can then use known parametrizations for neutrino spectra from decay of these particles in the Sun or Earth. The branching fractions for a specific set of parameters is shown in Fig. 1.

IV. NEUTRINO SPECTRA AND DETECTOR RATE

The neutrino spectra from annihilation events depend upon solar parameters, neutrino physics, quark hadronization [24], etc. Once we know the neutrino spectra from each of the decay products, the overall spectrum is given by convolving these spectra with the branching fractions. For the purposes of measurement in the neutrino telescopes, the relevant quantity is the detector rate. The technique for inferring the existence of the neutrino is observation of a muon, which is produced by a charged-current interaction. The cross section for this process is proportional to the energy of the neutrino, and the range of the subsequent muon is also proportional to its energy. Thus, we are interested in the second moment of the neutrino spectrum for the detector rate as a function of the injection energy ($E_{\rm in}$) [25,26]

$$\langle Nz^2\rangle_{F,i}(E_{\rm in}) = \int \left(\frac{dN}{dE}\right)_{F,i} (E_\nu, E_{\rm in}) \frac{E_\nu^2}{E_{\rm in}^2} dE_\nu \qquad (15)$$

The spectra from the Sun are more complicated than the Earth spectra. For the Earth, we consider the neutrino spectrum in the rest frame of the decaying particle, and then boost it for a particle with an energy $E_{\rm in}$. If the injected particle is a b or c quark, we also have to take hadronization into account. The quark loses energy as it hadronizes, so the injected energy is a fraction of $E_{\rm in}$. In the Solar case, we also have to consider the stopping of heavy hadrons. The core of the Sun is dense enough to slow b and c quarks further after hadronization. Another effect in the Sun is neutrino stopping and absorption. Neutrinos lose energy via neutral-current interactions and can be absorbed through charged-current interactions in the Sun. Stopping and absorption coefficients turn out to be different for neutrinos and antineutrinos. Hence, we expect a distinct spectrum for neutrinos and antineutrinos from the Sun. From the Earth, these spectra are identical. We produce the $\langle Nz^2\rangle$ plots in Fig. 2. Detailed numerical fits for these functions can be found in [27]. The combined detector rate is given by

$$\Gamma_{\rm detect} = c\left(\frac{\Gamma_A}{\rm s^{-1}}\right)\left(\frac{m_S}{\rm GeV}\right)^2 \sum_i a_i b_i \sum_F B_F \langle Nz^2\rangle_{F,i}(m_S). \qquad (16)$$

The sum over i is over neutrino and antineutrino states. The a_i are the neutrino scattering coefficients, $a_\nu = 6.8$, $a_{\bar\nu} = 3.1$. The b_i are the muon range coefficients, $b_\nu = 0.51$ and $b_{\bar\nu} = 0.67$. B_F is the annihilation branching fraction of the DMP for channel F.

For the sun, the constant $c = 2.54 \times 10^{-23}$ km^{-2} yr^{-1}. The expression for the detector rate for the Earth is scaled by the square of ratio of the Earth-Sun distance to the Earth radius. Thus, $c = 1.42 \times 10^{-14}$ km^{-2} yr^{-1} for the Earth.

The background for this process arises mainly from atmospheric neutrinos [27]. For the case of the Sun, we can reduce the background by including events only within a narrow angular cone along the line of sight from the detector to the Sun. There is also some background from the solar atmospheric neutrinos [28], where neutrinos are produced in the solar atmosphere by cosmic rays.

V. RESULTS

We have calculated the expected rate of detection in neutrino telescopes from these annihilations in the IDM. We restrict the parameter space to that allowed by relic abundance constraints by WMAP and other constraints discussed above. The IDM allows the Higgs mass to be higher than the standard electroweak precision test constraints [10], so we also analyze the signal for a 200 GeV SM Higgs boson. We do the calculation for different sets of

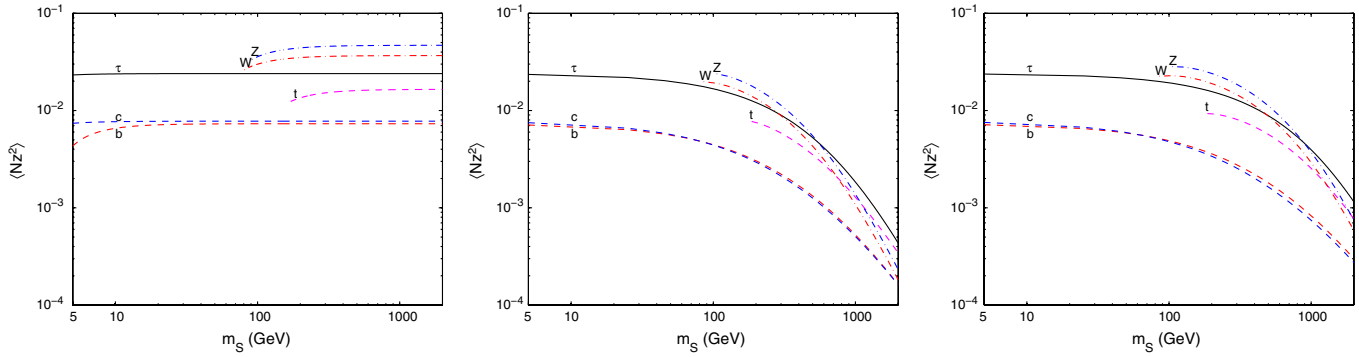

FIG. 2 (color online). Second moment of neutrino spectra from the Earth (left) and the Sun (center). Also shown is the second moment of antineutrino spectrum from the Sun (right). The Earth antineutrino spectrum is identical to the neutrino spectrum.

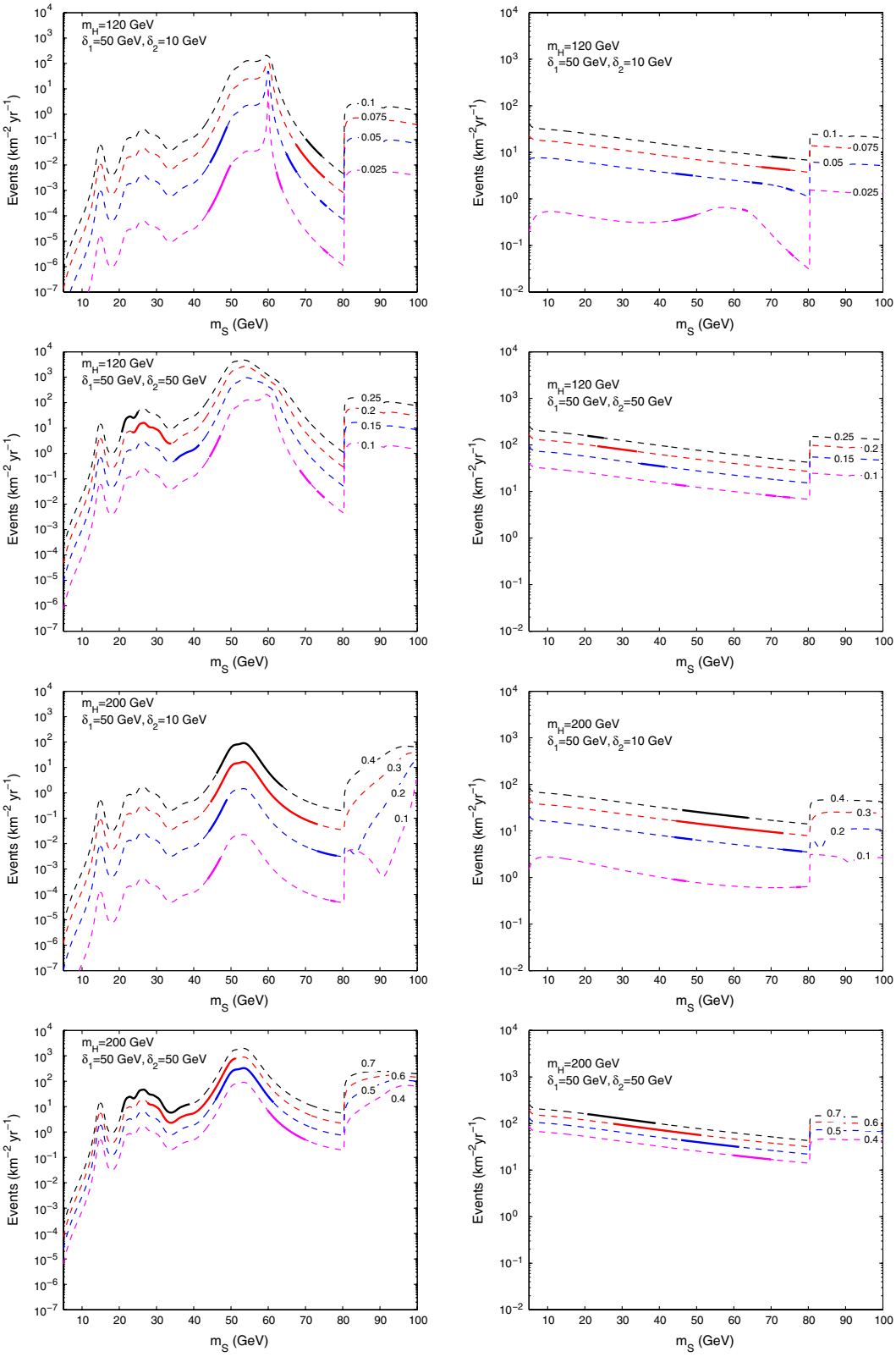

FIG. 3 (color online). Detector rate from annihilations in the Earth (left) and the Sun (right) in the low mass region for various values of λ_L. Different plots are for different Higgs masses and mass splittings (δ_1 and δ_2). The solid sections in the lines represent the mass range consistent with the correct relic abundance.

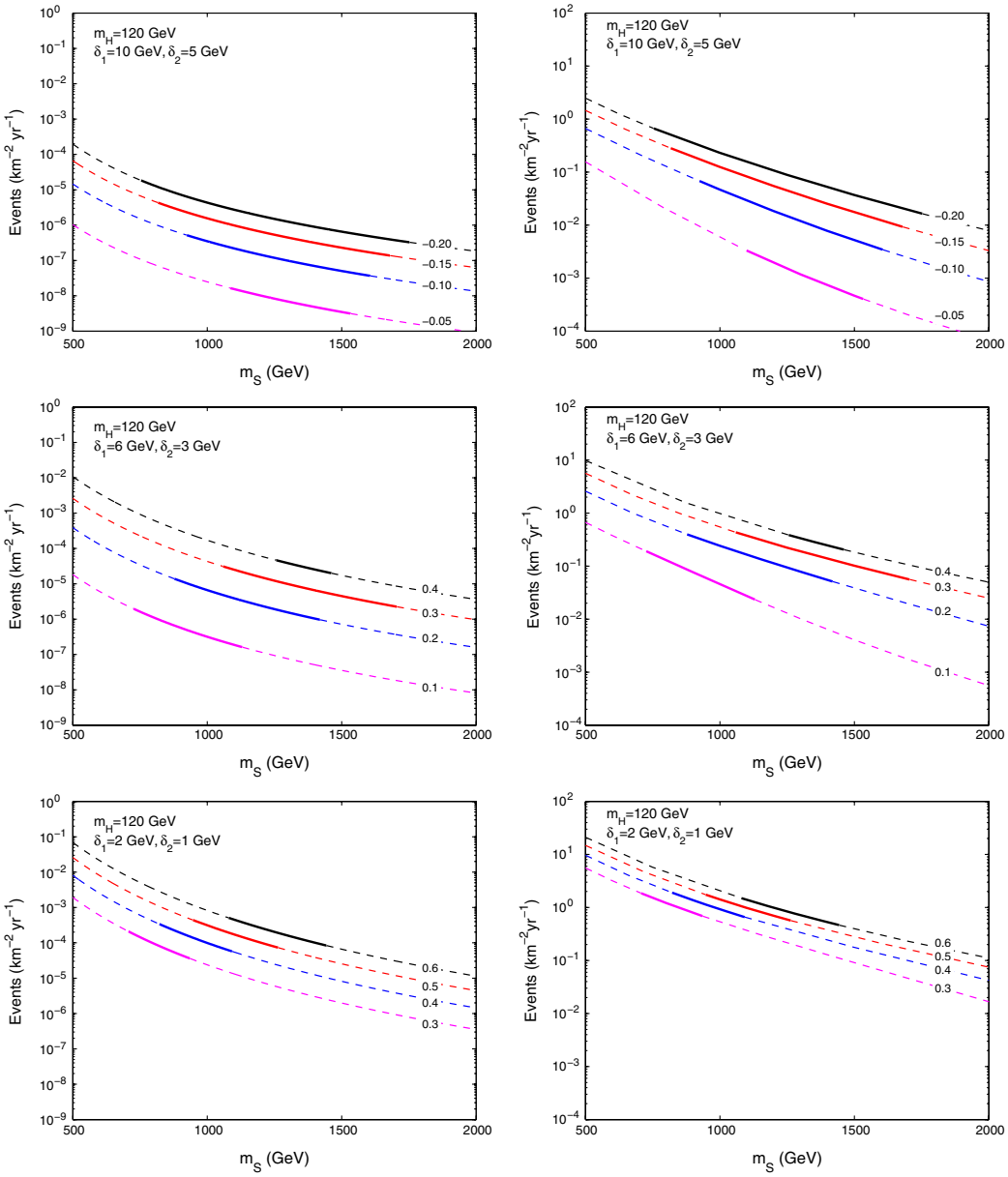

FIG. 4 (color online). Detector rate from annihilations in the Earth (left) and the Sun (right) in the high mass region for various values of λ_L. Different plots are for different mass splittings (δ_1 and δ_2). The solid sections in the lines represent the mass range consistent with the correct relic abundance.

mass splittings, δ_1 and δ_2. The plots are produced as a function of m_S for various values of λ_L. We find that the results are qualitatively different for the low mass ($m_S <$ 100 GeV) and the high mass (500 GeV $< m_S <$ 2 TeV) regions, hence we present them separately.

We plot the number of events observed per year in a detector with an effective area of 1 km^2, such as IceCube. The solid sections on the lines indicate the mass range which gives the correct relic abundance.

A. Low mass region

In the low mass region, the signals from the Earth and the Sun are comparable. The maximal signal for Earth is obtained around $m_S \simeq 50$ GeV. The various peaks in the Earth plots are explained by kinematics. When the DM mass is close to a nucleus mass there is no kinematic suppression [Eq. (11)]. As the DM mass increases, the cross section for DM capture decreases, leading to a reduction in the rate. In the Solar case, there is no kinematic resonance; therefore, the Earth signal exceeds the Solar signal at certain m_S values.

The branching fractions in the low mass region (below the W threshold), where annihilation products are quarks (b and c) and leptons (τ), are independent of λ_L. The detector rate depends on λ_L only through $\langle \sigma_A v \rangle$ and the capture rate (C) in this region.

We see up to ~100 events from the Earth with a 200 GeV Higgs boson and tens of events with a 120 GeV Higgs boson (Fig. 3). We expect to see as many as a few hundred events per year from the Sun in this parameter range.

B. High mass region

In the high mass region, the signal from Earth is suppressed by several orders of magnitude as compared to the signal from the Sun (Fig. 4). This is because the annihilation rate is not maximal (the capture and annihilation processes have not come into equilibrium) for the Earth, but it is for the Sun. The detector rate decreases with the mass of the dark matter particle, for both Earth and the Sun, due to the cross-sectional dependence on m_S and kinematic suppression. The branching fractions for the high mass particles have a nontrivial dependence on λ_L. Consequently, the qualitative features of the detector rate are influenced by the branching fractions and annihilation rate which, in turn, depend on the specific value of λ_L.

In this mass range, the signal from the Earth is too low to be observed. The signal from the Sun is more promising, and we expect to see a few events per year.

VI. CONCLUSION

Neutrino telescopes provide a very interesting mechanism for dark matter detection. With the increased sensitivity of IceCube, these signals can be used to test large ranges of parameter space in various models. We find a promising signal in the inert doublet model in two distinct parameter ranges. We get a few hundred events per year in the low mass region, and a few events from the Sun in the high mass region. For detection, a careful analysis of signal over background may be required.

ACKNOWLEDGMENTS

We thank Zackaria Chacko and Shufang Su for valuable discussions. E. M. D. is supported by the DOE under Grant No. DE-FG02-04ER-41298. P. A. and C. A. K. are supported by the NSF under Grant No. PHY-0801323.

[1] J. Ellis, J. S. Hagelin, D. V. Nanopoulos, K. Olive, and M. Srednicki, Nucl. Phys. **B238**, 453 (1984); K. Griest, Phys. Rev. D **38**, 2357 (1988).
[2] E. W. Kolb and R. Slansky, Phys. Lett. **135B**, 378 (1984).
[3] K. R. Dienes, E. Dudas, and T. Gherghetta, Nucl. Phys. **B537**, 47 (1999); G. Servant and T. M. P. Tait, Nucl. Phys. **B650**, 391 (2003).
[4] A. Birkedal-Hansen and J. G. Wacker, Phys. Rev. D **69**, 065022 (2004).
[5] J. Silk, K. Olive, and M. Srednicki, Phys. Rev. Lett. **55**, 257 (1985).
[6] H.-C. Cheng, J. L. Feng, and K. T. Matchev, Phys. Rev. Lett. **89**, 211301 (2002); D. Hooper and G. D. Kribs, Phys. Rev. D **67**, 055003 (2003).
[7] Z. Chacko, H.-S. Goh, and R. Harnik, J. High Energy Phys. 01 (2006) 108; H.-S. Goh and C. A. Krenke, Phys. Rev. D **76**, 115018 (2007).
[8] E. Ma, Phys. Rev. D **73**, 077301 (2006).
[9] N. G. Deshpande and E. Ma, Phys. Rev. D **18**, 2574 (1978).
[10] R. Barbieri, L. J. Hall, and V. S. Rychkov, Phys. Rev. D **74**, 015007 (2006).
[11] E. M. Dolle and S. Su, Phys. Rev. D **77**, 075013 (2008).
[12] D. Majumdar and A. Ghosal, Mod. Phys. Lett. A **23**, 2011 (2008).
[13] L. L. Honorez, E. Nezri, J. F. Oliver, and M. H. G. Tytgat, J. Cosmol. Astropart. Phys. 02 (2007) 028.
[14] M. Gustafsson, E. Lundstrom, L. Bergstrom, and J. Edsjo, Phys. Rev. Lett. **99**, 041301 (2007).
[15] E. Lundstrom, M. Gustafsson, and J. Edsjo, arXiv:0810.3924.
[16] D. N. Spergel *et al.*, Astrophys. J. Suppl. Ser. **170**, 377 (2007).
[17] G. Belanger, F. Boudjema, A. Pukhov, and A. Semenov, arXiv:0803.2360.
[18] A. Pukhov, arXiv:hep-ph/0412191.
[19] D. S. Akerib *et al.* (CDMS Collaboration), Phys. Rev. Lett. **96**, 011302 (2006).
[20] M. Shifman, A. Vainshtein, and V. Zakharov, Phys. Lett. **78B**, 443 (1978).
[21] J. Ellis, A. Ferstl, and K. A. Olive, Phys. Lett. B **481**, 304 (2000).
[22] A. Gould, Astrophys. J. **321**, 571 (1987).
[23] G. Jungman, M. Kamionkowski, and K. Griest, Phys. Rep. **267**, 195 (1996).
[24] T. K. Gaisser, G. Steigman, and S. Tilav, Phys. Rev. D **34**, 2206 (1986);
[25] M. Kamionkowski, Phys. Rev. D **44**, 3021 (1991).
[26] S. Ritz and D. Seckel, Nucl. Phys. **B304**, 877 (1988).
[27] V. Barger, W.-Y. Keung, G. Shaughnessy, and A. Tregre, Phys. Rev. D **76**, 095008 (2007).
[28] G. L. Fogli, E. Lisi, A. Mirizzi, D. Montanino, and P. D. Serpico, Phys. Rev. D **74**, 093004 (2006).